ISSN 1028-334X, Doklady Earth Sciences, 2018, Vol. 483, Part 1, pp. 1427–1430. © Pleiades Publishing, Ltd., 2018.
Original Russian Text © Yu.V. Bataleva, Yu.N. Palyanov, Yu.M. Borzdov, O.A. Bayukov, N.V. Sobolev, 2018, published in Doklady Akademii Nauk, 2018, Vol. 483, No. 1.

GEOCHEMISTRY

Experimental Modeling of C^0-Forming Processes Involving Cohenite and CO_2-Fluid in a Silicate Mantle

Yu. V. Bataleva[a,b,*], Yu. N. Palyanov[a,b], Yu. M. Borzdov[a,b], O. A. Bayukov[c], and Academician N. V. Sobolev[a,b]

Received March 16, 2018

Abstract—Experimental studies were performed in the Fe_3C–SiO_2–$(Mg,Ca)CO_3$ system (6.3 GPa, 1100–1500°C, 20–40 h). It is established that the carbide–oxide–carbonate interaction leads to the formation of ferrosilite, fayalite, graphite, and cohenite (1100 and 1200°C), as well as a Fe–C melt (1300°C). It is determined that the main processes in the system are decarbonation, redox-reactions of cohenite and a CO_2-fluid, extraction of carbon from carbide, and crystallization of metastable graphite (± diamond growth), as well as the formation of ferriferous silicates. The interaction studied can be considered as a simplified model of the processes that occur during the subduction of oxidized crustal material to reduced mantle rocks.

DOI: 10.1134/S1028334X18110016

According to the contemporary views, Fe carbide (cohenite, Fe_3C) may occur in reduced mantle rocks with total concentrations of carbon of more than 300 ppm at values of the oxygen fugacity that are at the iron–wustite buffer level or lower [1, 2]. In addition, it was demonstrated experimentally that cohenite may form under conditions of deep subduction in the case when the oxidized crustal material subsides into a metal-bearing mantle [1, 3]. The cohenite found in assemblage with diamond [4] is a direct demonstration of the presence of Fe in the mantle and indicates its involvement in the global carbon cycle and a potential genetic affinity with diamond. The stability of Fe carbide is determined by the reactions with the fO_2 -contrast minerals that can be brought during subduction [3, 5] and interactions with melts and fluids, the agents of mantle metasomatism. A CO_2-fluid, as well as carbonate-bearing melts, is considered as the most likely oxidative metasomatic agent that can be generated under subduction conditions [6–8]. The possibility of redox interaction between Fe carbide and oxidative agents, which potentially leads to the formation of diamond or graphite, is considered in the data on diamond inclusions with the compositions varying from strongly reduced (Fe^0, Fe_3C, SiC) [4, 9, 10] to oxidized (CO_2, carbonates) [10, 11].

The analysis of the current state of the problem shows that experimental studies on the reconstruction of scenarios of Fe carbide interaction with mantle minerals, melts, and fluids under different fO_2 conditions are performed infrequently. At present, experiments have been conducted on modeling the interactions of carbide with sulfur-bearing mantle fluids and melts [12], as well as with fO_2 contrast phases, carbonates, and oxides [3, 5]. The purpose of this work is experimental modeling of carbon-forming reactions of carbide-and-CO_2-fluid interaction in the presence of mantle silicates, orthopyroxene, and olivine, and determination of the potential mechanisms of graphite (diamond) formation during this interaction.

The experimental studies were performed in the Fe_3C–SiO_2–$(Mg,Ca)CO_3$ (carbide–oxide–carbonate) system using the BARS multianvil high-pressure split-sphere apparatus [13] at 6.3 GPa, 1100–1500°C for 20–40 h. As initial reagents, we used natural magnesite, dolomite (<0.5% wt of admixtures; the Satka deposit), and preliminarily synthesized Fe_3C and SiO_2 (<0.01% wt of admixtures). The mass proportions of the initial substances were 30 mg of Fe_3C, 36 mg of SiO_2, 13.4 mg of $MgCO_3$, and 3.4 mg of $CaMg(CO_3)_2$. Taking into account the previous experience of work with high-ferriferous phases at the mantle P and T [5, 12], we selected graphite as the optimal ampule material. The ground (up to 20–30 μm) and thoroughly mixed initial reagents were placed in the graphite ampules; however, a part of the carbide was not ground and was placed in the ampule as crystals 300–

[a] *Sobolev Institute of Geology and Mineralogy, Siberian Branch, Russian Academy of Sciences, Novosibirsk, 630090 Russia*
[b] *Novosibirsk State University, Novosibirsk, 630090 Russia*
[c] *Kirensky Institute of Physics, Siberian Branch, Russian Academy of Sciences, Krasnoyarsk, 660036 Russia*
**e-mail: bataleva@igm.nsc.ru*

Table 1. Compositions of silicate phases obtained in the carbide–oxide–carbonate system at 6.3 GPa

Exp. no.	T, °C	Phase	N_A	Composition, wt %					n(O)	Formula units				
				SiO_2	FeO	MgO	CaO	Sum		Si	Fe	Mg	Ca	Sum
OC-19	1100	OPx	15	$49_{(1)}$	$43_{(3)}$	$7_{(1)}$	$1.0_{(8)}$	99.7	6	$2.02_{(5)}$	$1.5_{(1)}$	$0.4_{(1)}$	$0.04_{(3)}$	3.98
		Ol	15	$29.1_{(5)}$	$64.1_{(5)}$	$6.2_{(1)}$	$0.2_{(1)}$	99.72	4	$0.96_{(1)}$	$1.76_{(2)}$	$0.31_{(0)}$	$0.01_{(1)}$	3.04
OC-96	1200	OPx	12	$48_{(2)}$	$43_{(3)}$	$7_{(3)}$	$1.0_{(7)}$	99.62	6	$2.01_{(2)}$	$1.5_{(2)}$	$0.4_{(2)}$	$0.03_{(2)}$	3.99
		Ol	14	$30.3_{(8)}$	$63_{(3)}$	$4_{(3)}$	$0.8_{(8)}$	99.62	4	$1.00_{(1)}$	$1.7_{(1)}$	$0.2_{(1)}$	$0.03_{(2)}$	3.00
OC-97	1300	OPx	12	$49.8_{(1)}$	$36.3_{(9)}$	$11.9_{(8)}$	$1.5_{(1)}$	$99.6_{(2)}$	6	$2.00_{(1)}$	$1.22_{(4)}$	$0.72_{(4)}$	$0.06_{(0)}$	$4.00_{(1)}$
		Ol	10	$32.0_{(5)}$	$56_{(1)}$	$11.0_{(5)}$	$0.07_{(1)}$	$99.6_{(2)}$	4	$1.00_{(1)}$	$1.48_{(4)}$	$0.52_{(2)}$	–	$3.00_{(1)}$
OC-10	1400	OPx	10	$49.6_{(9)}$	$36_{(2)}$	$12_{(2)}$	$1.5_{(10)}$	$99.5_{(3)}$	6	$1.99_{(1)}$	$1.20_{(9)}$	$0.7_{(1)}$	$0.06_{(4)}$	$4.01_{(1)}$
		Ol	8	$32.1_{(3)}$	$55.6_{(6)}$	$12.0_{(2)}$	–	$99.7_{(2)}$	4	$1.00_{(1)}$	$1.44_{(0)}$	$0.56_{(1)}$	–	$3.00_{(1)}$
OC-93	1500	OPx	16	$48.9_{(5)}$	$38.8_{(7)}$	$10.3_{(9)}$	$1.6_{(4)}$	$99.6_{(3)}$	6	$1.99_{(1)}$	$1.32_{(4)}$	$0.63_{(5)}$	$0.07_{(2)}$	$4.01_{(1)}$
		Ol	10	$32.3_{(1)}$	$55.6_{(8)}$	$11.8_{(8)}$	–	$99.8_{(2)}$	4	$1.00_{(0)}$	$1.44_{(1)}$	$0.55_{(1)}$	–	$2.99_{(1)}$

Opx, orthopyroxene; Ol, olivine; N_A, number of analyses; n(O), number of oxygen atoms. The value of standard deviation for the last sign is given in parentheses.

500 μm in size. The seed diamond crystals of cubic-octahedral habitus (500 μm) were added to the reaction volume of the ampules to obtain additional information on possible diamond crystallization.

The phase and chemical compositions of the samples obtained were determined by the methods of energy-dispersive microscopy (a Tescan MIRA3 LMU scanning electron microscope) and by microprobe analysis (Camebax-micro). The research into the phase relationships in the samples, as well as the study of the micromorphology of the seed diamond crystals were done by the method of scanning electron microscopy. The analytic research was carried out at the Center for Collective Use of Multi-element and Isotopic Analysis, Siberian Branch, Russian Academy of Sciences. The composition of iron-bearing phases, the valent state of valent state of Fe therein, and the distribution of Fe in the phases and nonequivalent positions was determined by the method of Mössbauer spectroscopy; the measurements were made at a room temperature using an MC-1104Em spectrometer with a Co^{57}(Cr) source.

Table 1 presents the parameters and compositions of the phases obtained. It is established that at the lowest temperatures (1100–1200°C, t = 30–40 h) as a result of carbide–oxide–carbonate interaction, graphite forms in the assemblage with orthopyroxene, cohenite, and coesite. Graphite forms at the place of initial large carbide crystals (Fig. 1a); however, it is also present in small quantities in the interstices of a silicate matrix represented by a polycrystalline aggregate of orthopyroxene and olivine. On the seed diamond crystals, there are no visible changes at 1100–1400°C (no traces of growth or dissolution). The silicates obtained are characterized by high ferruginosity and represent ferrosilite (~$Fe_{1.5}Mg_{0.4}Ca_{0.04}Si_2O_6$) and fayalite (~$Fe_{1.76}Mg_{0.31}Ca_{0.01}SiO_4$). The Mössbauer spectroscopic analysis of the samples obtained showed that ferrosilite contains Fe^{3+}; in which case, the values of $Fe^{3+}/\Sigma Fe$ amount to ~0.08. The Fe distribution between the phases obtained is displayed in Fig. 2.

At 1300 and 1400°C, as a result of carbide–oxide–carbonate interaction, graphite is formed in the assemblage with orthopyroxene and olivine, and an iron–carbon melt is also formed. According to the calculations of the mass balance, the weight proportions of orthopyroxene, olivine, graphite, and a Fe–C melt are 63 : 31 : 5 : 1. In the polycrystalline aggregate of pyroxene ($Fe_{1.2}Mg_{0.7}Ca_{0.1}Si_2O_6$), singular microspheres of the quenched Fe–C melt (10–20 μm) are located, which are spatially confined to relatively large crystals of graphite (~30–150 μm), olivine (~30–50 μm), and also a fine-crystalline aggregate+olivine aggregate (Fig. 1b). The inclusions of the quenched Fe–C melt and graphite were recorded in the orthopyroxene crystals. The quenched iron–carbon melt is an aggregate of the Fe^0 and Fe_3C microdendrites. The total concentration of carbon in this melt is 4.5–5.5% wt. The olivine composition corresponds to $Fe_{1.5}Mg_{0.5}SiO_4$ (1300°C) and ($Fe_{1.4}Mg_{0.6}SiO_4$). At 1500°C, graphite formed in the assemblage with orthopyroxene and olivine (Fig. 1c); we also noticed a layer grown on the seed diamond crystals. There was no Fe–C melt in the reaction volume. Orthopyroxene was represented by the large prismatic crystals 150–200 μm in size, and its composition was $Fe_{1.3}Mg_{0.6}Ca_{0.1}Si_2O_6$. The study of the samples obtained at 1300–1500°C by the method of Mössbauer spectroscopy showed that the silicate phases contained only Fe^{2+}. The crystals of orthopyroxene included a quenched Fe–C melt and graphite. As in the case of lower temperatures, olivine and

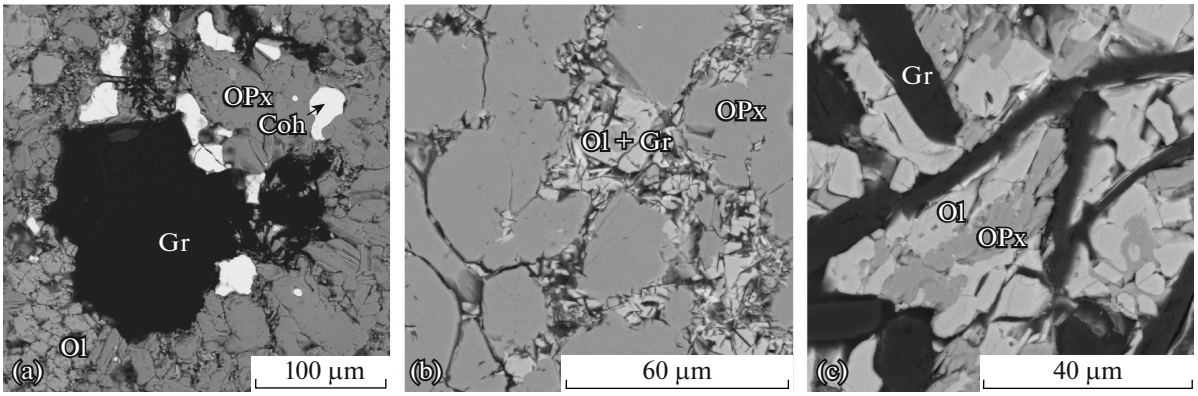

Fig. 1. SEM-microphotos of the polished fragments of the samples obtained in the carbide–oxide–carbonate system (6.3 GPa, 1100–1500°C): (a) graphite and cohenite in a polycrystalline aggregate of orthopyroxene and olivine (1200°C); (b) the aggregate of a large orthopyroxene crystals with olivine and graphite in interstices (1400°C); (c) the polycrystalline aggregate of orthopyroxene, olivine, and graphite (1500°C). Here and in Fig. 2, OPx, orthopyroxene; Ol, olivine; Gr, garnet; Coh, cohenite.

graphite were situated in the interstices of a polycrystalline aggregate of orthopyroxene.

The reconstruction of the processes of the carbide–oxide–carbonate interaction showed that at 1100 and 1200°C the system is fully decarbonated, which results in the formation of orthopyroxene and olivine and a release of a CO_2-fluid (1), (2), which in turn enters the redox interaction with Fe carbide (3):

$$2(Mg,Ca)CO_3 + 2SiO_2 \rightarrow (Mg,Ca)_2Si_2O_6 + 2CO_2, \quad (1)$$

$$2MgCO_3 + SiO_2 \rightarrow Mg_2SiO_4 + 2CO_2, \quad (2)$$

$$2Fe_3C + 3CO_2 \rightarrow 6FeO_{\text{in silicates}} + 5C^0. \quad (3)$$

The formation of elemental carbon (graphite) and FeO, which does not form an independent phase, but constitutes a part of silicates by the resulting reaction (presented schematically), occurs during this interaction:

$$2(Mg,Ca)CO_3 + 4SiO_2 + 2Fe_3C \rightarrow (Fe,Mg,Ca)_2Si_2O_6 + 2(Fe,Mg)_2SiO_4 + 2/3Fe_3C + 3C^0. \quad (4)$$

At the higher temperatures of the carbide–oxide–carbonate interaction, in addition to reactions (1)–(3), a Fe–C melt forms:

$$3Fe_3C + 3CO_2 \rightarrow 6FeO_{\text{in silicates}} + 3Fe{-}C_{\text{melt}} + 5C^0. \quad (5)$$

It is most likely that the new portions of the CO_2-fluid forming during the system decarbonation enter into a redox interaction with the Fe–C melt, which results in its total oxidation accompanied by the formation of ferriferous orthopyroxene, olivine, graphite, and diamond growth on the seed crystals (1500°C):

$$3Fe{-}C_{\text{melt}} + 3CO_2 \rightarrow 6FeO_{\text{in silicates}} + 4C^0. \quad (6)$$

The typical features of graphite formation and diamond growth in the carbon-forming processes resulted from parallel reactions of decarbonatization and redox interaction of the CO_2-fluid and Fe carbide are determined experimentally. This redox interaction can be considered as a basis for the reconstruction of the mechanism of graphite formation at 1100–1500°C. It was established that the formation of graphite from carbide carbon occurs when cohenite is oxidized to FeO and is accompanied by carbon extraction from Fe_3C. The process of coheite oxidation by the CO_2-fluid occurs simultaneously with the reduction of CO_2 to C^0, which leads to crystallization of metastable graphite with a carbonate source. The intergrain

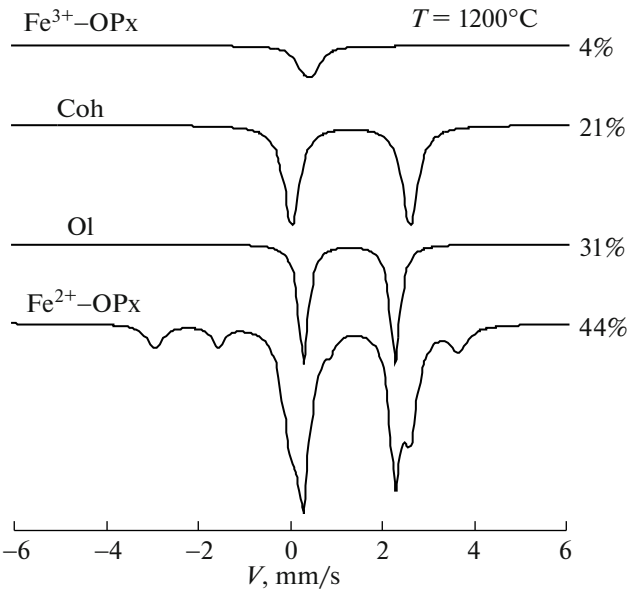

Fig 2. Mössbauer spectra of the sample obtained at 1200°C.

CO_2-fluid is the most likely medium for graphite formation by this mechanism. It was established that, at higher temperatures, in addition to the above mechanism, graphite formation and diamond growth on the seed crystals (1500°C) occur as a result of full oxidation of the Fe–C melt by the fluid, which is accompanied by the formation of a FeO-component in silicates and the corresponding reduction of the CO_2-fluid to C^0. It is most likely that the media for graphite crystallization and diamond growth by this mechanism at the different stages of crystallization are the intergrain fluid and the Fe–C melt, and the carbon sources are carbide and carbonate. The dominant formation of graphite rather than diamond in these media under the parameters of the experimental study can be associated with the different diamond-forming fluid capacity [14] and the inhibiting action of oxygen-bearing admixtures in the metal–carbon media [15].

The studied interaction of Fe carbide with oxides and carbonates can be considered as a simplified model of processes that occur during the subduction of an oxidized crustal material to the reduced mantle rocks; however, the main established regularities and the mechanisms of graphite (±diamond) formation can also be used for more complex natural systems. It is known that decarbonation is one of the most frequent fluid-generating processes under conditions of subduction, the P–T parameters of which vary in a wide range. It has been found that the participation of Fe carbide in these processes leads to the implementation of a set of carbon-forming processes that include extraction of carbon from cohenite and reduction of a CO_2-fluid to C^0 and lead to the formation of graphite (±diamond growth) in the association with ferriferous silicates. The data obtained expand the existing views of the possible processes of the global carbon cycle with the participation of Fe carbides, as well as the processes of graphite crystallization (±diamond growth) under subduction conditions.

ACKNOWLEDGMENTS

This work was supported by the Russian Foundation for Basic Research (project no. 16–35–60024) and was performed as part of a State Assignment (project no. 0330–2016–0007).

REFERENCES

1. A. Rohrbach and M. W. Schmidt, Nature **472**, 209–212 (2011).
2. B. Marty, Earth Planet. Sci. Lett. **313–314**, 56–66 (2012).
3. Y. N. Palyanov, Y. V. Bataleva, Y. M. Borzdov, et al., Proc. Natl. Acad. Sci. U. S. A. **110** (51), 20408–20413 (2013).
4. D. E. Jacob, A. Kronz, and K. S. Viljoen, Contrib. Mineral. Petrol. **146** (5), 566–576 (2004).
5. Yu. V. Bataleva, Yu. N. Pal'yanov, Yu. M. Borzdov, et al., Russ. Geol. Geophys. **57** (1), 176–189 (2016).
6. R. W. Luth, in *Reference Module in Earth Systems and Environmental Sciences, Treatise on Geochemistry* (Elsevier, 2014), pp. 355–391.
7. I. D. Ryabchikov, Dokl. Earth Sci. **429** (8), 1346–1349 (2009).
8. L. N. Kogarko, Geochem. Int. **44** (1), 3–10 (2006).
9. N. V. Sobolev, E. S. Efimova, and L. N. Pospelova, Geol. Geofiz., No. 12, 25–28 (1981).
10. T. Stachel, J. W. Harris, and G. P. Brey, Contrib. Mineral. Petrol. **132**, 34–47 (1998).
11. M. Schrauder and O. Navon, Nature **365**, 42–44 (1993).
12. Y. V. Bataleva, Y. N. Palyanov, Y. M. Borzdov, et al., Lithos **286–287**, 151–161 (2017).
13. Y. N. Palyanov, Y. M. Borzdov, A. F. Khokhryakov, et al., Cryst. Growth Des. **10**, 3169–3175 (2010).
14. Yu. N. Pal'yanov, A. G. Sokol, A. F. Khokhryakov, et al., Dokl. Earth Sci. A **375** (9), 1395–1398 (2000).
15. Y. N. Palyanov, A. F. Khokhryakov, Y. M. Borzdov, et al., Cryst. Growth Des. **13** (12), 5411–5419 (2013).

Translated by L. Mukhortova